

Density Functional Theory Study on the Cycloaddition of Carbon Dioxide with Propylene Oxide Catalyzed by Alkylmethylimidazolium Chlorine Ionic Liquids

Hui Sun and Dongju Zhang*

Key Lab of Colloid and Interface Chemistry, Ministry of Education, School of Chemistry and Chemical Engineering, Shandong University, Jinan 250100, People's Republic China

Received: May 19, 2007; In Final Form: June 13, 2007

The cycloaddition of carbon dioxide (CO₂) with propylene oxide (PO) in the absence and presence of alkylmethylimidazolium chloride ([C_nmim]Cl, *n* = 2, 4, and 6) ionic liquids has been studied in detail by performing density functional theory calculations at the B3PW91/6-31G(d,p) level. It is found that in the absence of [C_nmim]Cl the reaction proceeds via two possible channels (each of them involves one elementary step) and the corresponding barriers are found to be as high as 59.71 and 55.10 kcal mol⁻¹, while in the presence of [C_nmim]Cl there exist five possible reaction channels (each of them involves two or three elementary steps) and the barriers of the rate-determining steps are reduced to 27.93–38.05 kcal mol⁻¹, clearly indicating that [C_nmim]Cl promotes the reaction via modifying the reaction mechanism and thereby remarkably decreases the barrier. The origination of the catalytic activity of [C_nmim]Cl has been analyzed in detail. The present theoretical study rationalizes the early experimental findings well and provides a clear profile for the cycloaddition of CO₂ with PO promoted by [C_nmim]Cl.

1. Introduction

Room-temperature ionic liquids (RTILs), a new class of liquids that are entirely composed of ions, are now widely recognized as an important component of green chemistry. This is mainly attributed to their remarkable characteristics,^{1–3} including negligible vapor pressure, excellent thermal and chemical stabilities, nonflammability, and good reusability. Moreover, they also have low melting point, powerful solvent capacity for many organic, inorganic, and organometallic compounds, and wide liquid range up to 300 °C. The majority of RTILs reported in the literatures are tetraalkylammonium salts, tetraalkylphosphonium salts, 1,3-dialkylimidazolium salts, and *N*-alkylpyridinium salts. In the early research, RTILs were generally used as environmentally friendly alternatives to volatile organic media in organic synthesis.^{4–6} Later, RTILs were found to show excellent catalytic activity for many important chemical reactions, such as Michael addition,⁷ Beckmann rearrangement,⁸ and Henry reaction,⁹ since Wilkes and co-workers¹⁰ reported the first successful use of dialkylimidazolium chloroaluminate as a catalyst in Friedel–Crafts acylations in 1986. Currently, RTILs are receiving growing attention due to their advantages as reagents and catalysts with tunable features for various targeted chemical tasks.^{11–13} In particular, imidazolium-based ionic liquids present more rapidly increasing importance in the area of catalysis. A number of chemical reactions catalyzed by various task-specific (or functional) dialkylimidazolium ionic liquids have been reported.^{14–17} While substantial and extensive efforts have been devoted to developing new RTILs for catalytic applications, not much is known about the detailed reaction mechanism. To better understand the catalysis of RTILs on many important organic synthesis reactions, such as Diels–Alder reactions, Markovnikov additions, and Heck reactions, we have recently launched a theoretical project, which aims to address the microscopic details on how RTILs influence chemical reactivity and selectivity, based on quantum chemical calculations, and some prototypes have been reported.^{18,19}

In this paper, we carry out our notion on an important class of reactions, the cycloaddition of carbon dioxide (CO₂) with epoxides to synthesize five-membered cyclic carbonates, which

are extensively used as high-polarity solvents, electrolytes for batteries, efficient protecting groups in carbohydrate chemistry, and raw materials in a wide range of chemical reactions.^{20,21} Propylene oxide (PO) is chosen as a prototype of epoxides for study. This work was inspired by the extraordinary success of the cycloaddition of CO₂ with PO in alkylmethylimidazolium chloride ionic liquids (denoted as [C_nmim]Cl, *n* = 2, 4, and 6).^{22–24}

CO₂ is one of the most important greenhouse gases, which has resulted in global warming effects and serious environmental problems. On the other hand, CO₂ can be used as an abundant, inexpensive, nonflammable, and nontoxic carbon resource to produce useful organic compounds. One of the most widely applied technologies for the fixation and utilization of the carbon resource is the cycloaddition of CO₂ with epoxides to afford five-membered cyclic carbonates. So far, quite numerous catalytic processes about the cycloaddition have been reported.^{25–33} However, most of the catalysts reported in the literatures, such as metal halides,^{25,26} metal oxides,^{27,28} organometallic compounds,^{29–31} Lewis acid/bases,³² and zeolites,³³ usually suffer from low catalyst activity or need additional cosolvent or high pressures/temperatures, limiting their practicality. Thus, developing new catalysts for this cycloaddition reaction is highly desirable. Recently, some pure imidazolium-based ionic liquids with different alkyl groups and anions were found to remarkably promote the reaction.^{22–24} For example, Park et al.²⁴ recently realized efficiently the copolymerization of allyl glycidyl ether and CO₂ in alkylmethylimidazolium-based ionic liquids with anions Cl⁻, BF₄⁻, and PF₆⁻ under 140 psig for 48 h at 100 °C. It was found from these experiments that (i) there was no detectable conversion of epoxide if no RTILs were used, (ii) the selectivity of the desired five-member cyclic carbonate in the presence of RTILs was quite high (nearly 100%), (iii) the yield of cyclic carbonate increased with lengthening alkyl chain, and (iv) the recycle times of catalysts remarkably increased. Although the cycloaddition reaction has been successfully achieved,^{22–24} the details of the mechanism are still ambiguous and worthy of further exploration. Herein, by performing density functional theory (DFT) calculations, we show the details of mechanism for the cycloaddition reaction of CO₂ and PO with and without the presence of [C_nmim]Cl (*n* = 2, 4 and 6), and

* Corresponding author: e-mail zhangdj@sdu.edu.cn.

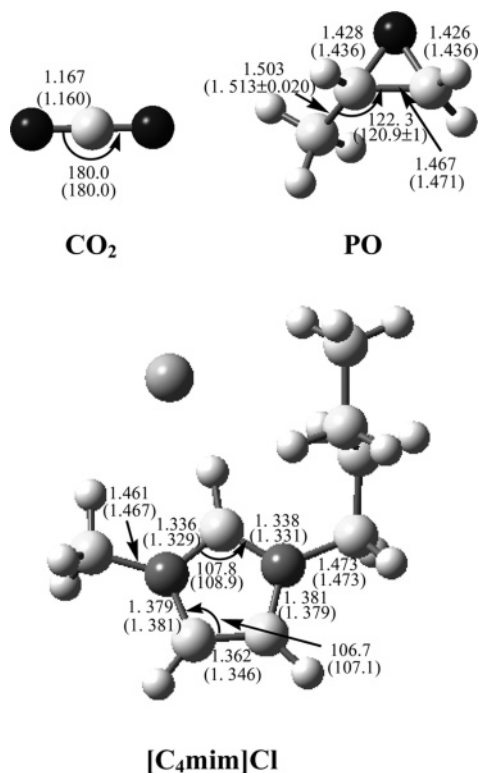


Figure 1. Optimized geometries for CO₂, PO, and [C₄mim]Cl. Distances are in angstroms and angles are in degrees. The values in parentheses are experimental results from refs 49–51.

we expect to provide a reasonable explanation for the experimental observations.

2. Computational Details

Our calculations were carried out by performing density functional theory (DFT)^{34–37} calculations by use of the B3PW91 functional^{37,38} with the 6-31G(d,p) basis set as implemented in Gaussian 03 program package.³⁹ The B3PW91 functional has been proven to give more reliable intermolecular interaction energy than other functionals, such as the most popular B3LYP functional, for complexes involving strongly bound ionic hydrogen bonds.⁴⁰ The systems involving RTILs were demon-

strated to involve electrostatic and hydrogen-bond interactions.^{41–45} So it is expected that the B3PW91 functional would give a reasonable description for the present cycloaddition reaction promoted by [C_nmim]Cl. The combination of B3PW91 functional with the medium-size 6-31G(d,p) basis set offers a good compromise between computational cost and accuracy of computational outcomes. All geometries for the isolated reactants, products, intermediates, and transition states involved in the cycloaddition reaction have been fully optimized. Vibrational frequency calculations, from which the zero-point energies (ZPEs) were derived, have been performed for each optimized structure at the same level to identify the natures of all the stationary points (local minimum or first-order saddle point). The intrinsic reaction coordinate (IRC)⁴⁶ pathways have been traced in order to verify that each saddle point links two desired minima. The electronic properties for the reactants were illustrated on the basis of the natural bond orbital (NBO) analysis.^{47,48} For all the cited energies, the ZPE corrections have been taken into account.

To support our choice for the functional and basis set, we first performed benchmark calculations for isolated CO₂, PO, and [C₄mim]Cl molecules, for which experimental geometrical parameters are available.^{49–51} Figure 1 compares the calculated results with the experimental values. We find that the optimized geometrical parameters are in good agreement with the experimental values, and the deviations are only 0.00–0.02 Å for the bond lengths and 0.4–1.3° for the bond angles, indicating the reliability of the calculation method used for describing the present system.

3. Results and Discussion

3.1. Cycloaddition Reaction in the Absence of [C_nmim]Cl.

To make a quantitative comparison with the catalyzed reaction, we first consider the cycloaddition of CO₂ with PO in the absence of [C_nmim]Cl. Figure 2 shows the calculated potential energy surface (PES) profiles along the reaction coordinate with the optimized structures of the minima and transition states involved in the reaction.

Initially, a dimolecular complex between CO₂ and PO, denoted as IM, was formed via the weak van der Waals interaction, as indicated by the long distance (2.853 Å) and small binding energy (1.66 kcal mol⁻¹) between two molecules. Starting from IM, two structurally very similar five-membered ring transition states, TS1 and TS2, have been located on the

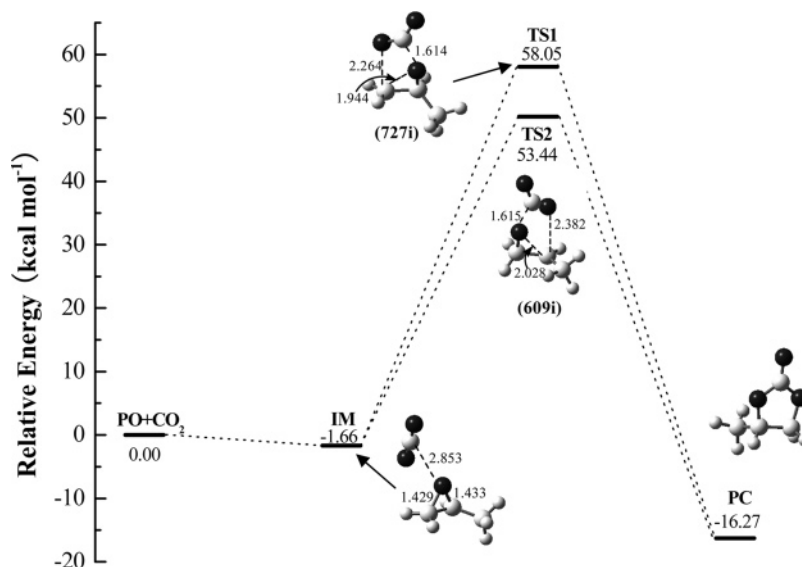


Figure 2. Potential energy surface (PES) profiles with the optimized geometries of stable points (intermediate, transition states, and product) on PESs for the cycloaddition reaction of CO₂ with PO in the absence of [C_nmim]Cl. Values in parentheses denote the imaginary frequencies of transition states. Distances are in angstroms.

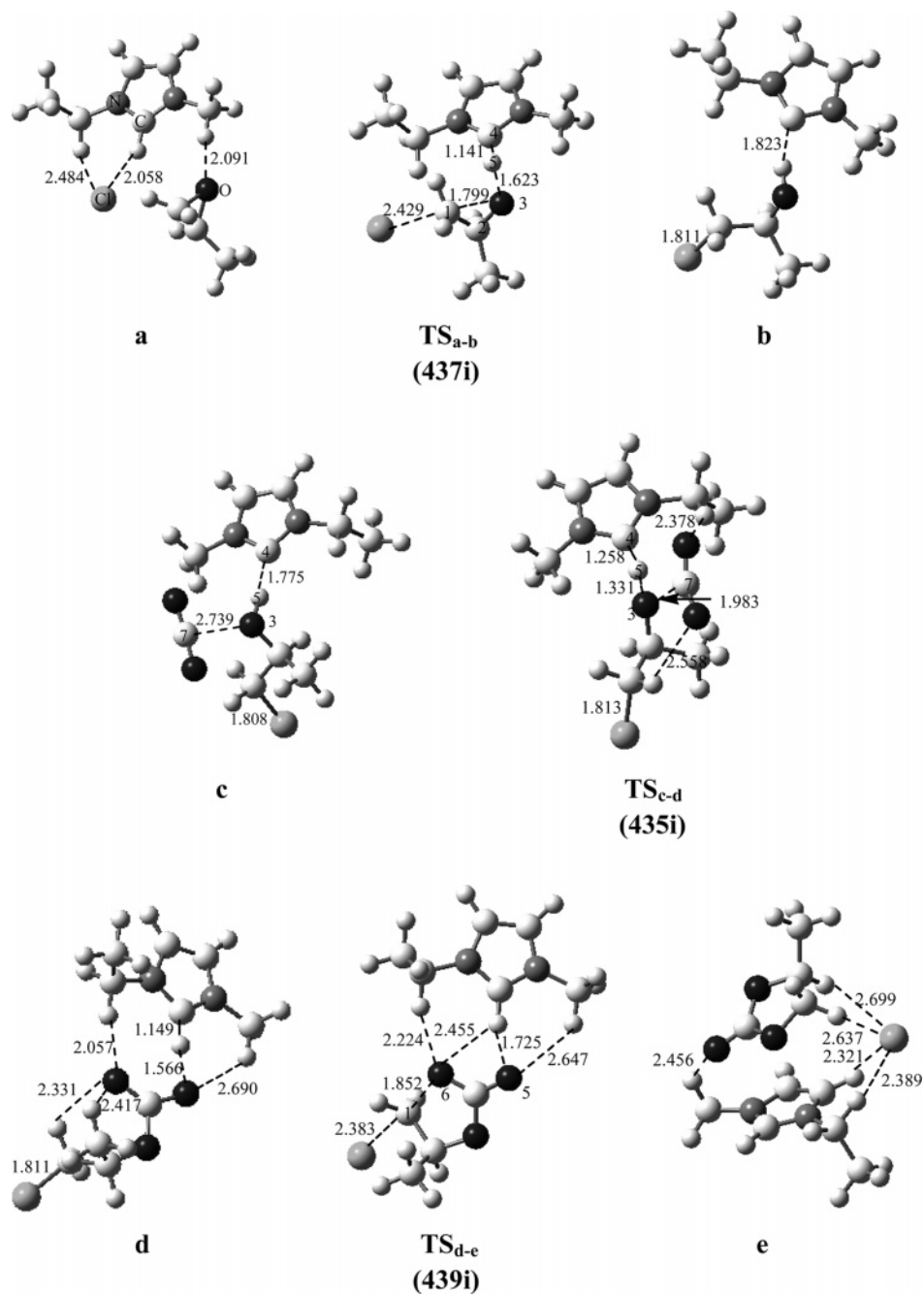


Figure 3. Optimized geometries for the intermediates and transition states involved in path I. Values in parentheses denote the imaginary frequencies of transition states. Distances are in angstroms.

PES, where one of the C–O bonds in PO is breaking and the two C–O bonds between PO and CO₂ are forming. In TS1 the breaking C–O bond is elongated to 1.944 Å and the two forming C–O bonds are shortened to 1.614 and 2.264 Å, while the corresponding ones in TS2 are 2.028, 1.615, and 2.382 Å, respectively. The unique imaginary frequencies of TS1 and TS2 are 727i and 609i cm⁻¹, respectively, and the corresponding normal modes clearly indicate that in both cases the cycloaddition reaction proceeds via a concerted mechanism. Along the reaction coordinate, our forward IRC calculations demonstrate that both TS1 and TS2 converge to the desired product, propylene carbonate (PC), which is 16.27 kcal mol⁻¹ more stable than the isolated reactants, indicating that the cycloaddition reaction is thermodynamically favorable. However, the barriers from IM to TS1 and TS2 are found to be as high as 59.71 and 55.10 kcal mol⁻¹, respectively, which may account for the observed difficulty of the cycloaddition reaction in the absence of catalyst [C_nmim]Cl.

3.2. Cycloaddition Reaction in the Presence of [C_nmim]-Cl. In this section, we turn to the cycloaddition reaction in the presence of [C_nmim]Cl. [C₂mim]Cl was chosen as a representative of [C_nmim]Cl (*n* = 2, 4, and 6) to study the mechanism details. By performing extensive PES scans, we found that there exist five possible pathways I–V for the reaction in the presence of [C₂mim]Cl, which can be divided into two sets: the three-step mechanism for paths I and II, and the two-step mechanism for paths III–V. The structures of the stable points located on each path, with the main geometrical parameters, are shown in Figures 3–6. The PES profiles along the reaction coordinate are depicted in Figure 7, where the sum of the energies of the isolated reactants (CO₂ + PO) and catalyst ([C₂mim]Cl) is taken as zero energy. In the following sections, we will discuss the geometries and energies of all intermediates and transition states involved in paths I–V in detail.

As shown in Figure 7, path I involves three elementary steps. Figure 3 shows the optimized structures for all intermediates

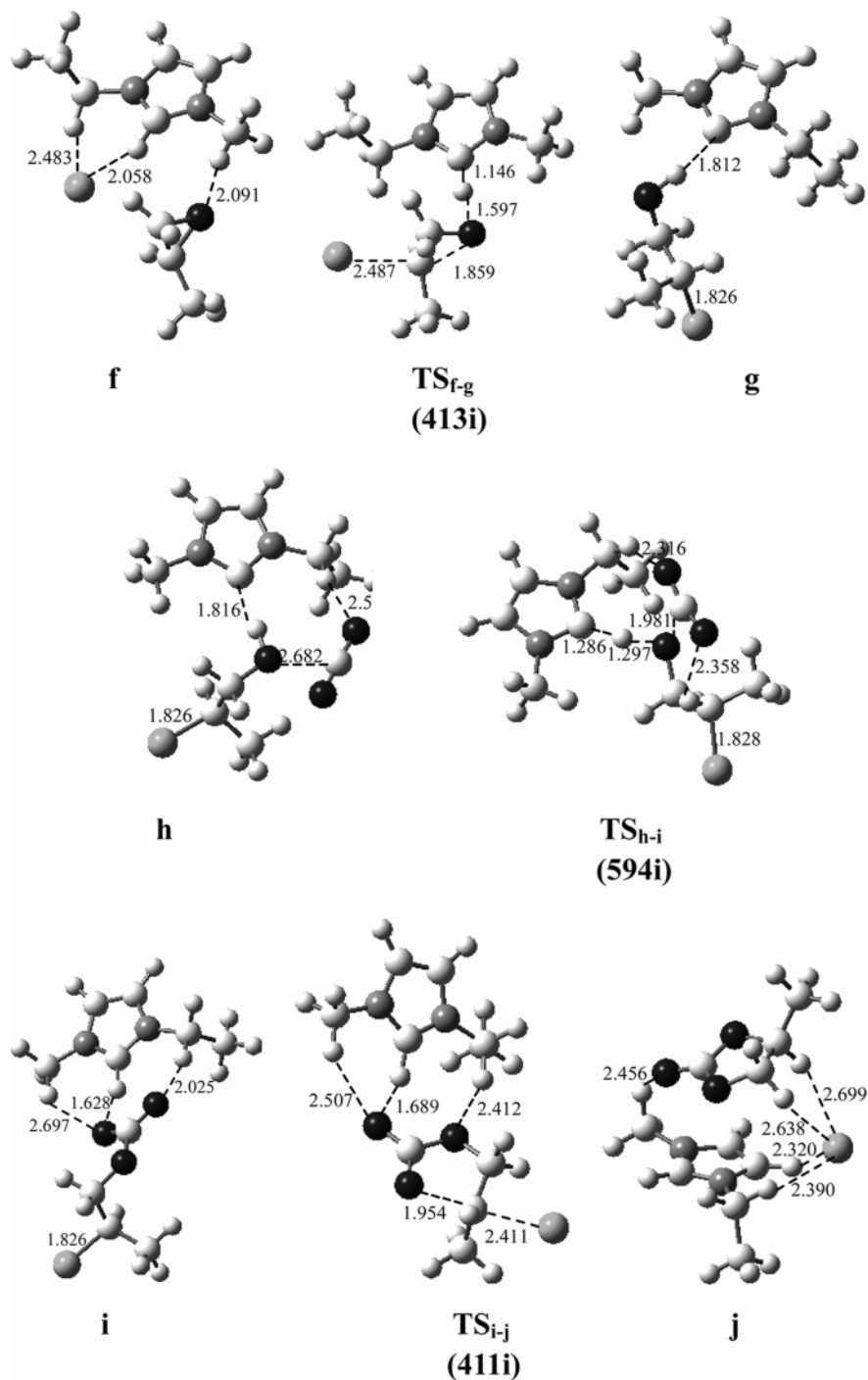


Figure 4. Optimized geometries for the intermediates and transition states involved in path II. Values in parentheses denote the imaginary frequencies of transition states. Distances are in angstroms.

and transition states involved in this pathway. Initially, PO and [C₂mim]Cl interact via hydrogen bond to form a supermolecule complex, a, which lies 7.06 kcal mol⁻¹ lower in energy than the isolated reactants. And then this complex can be converted into intermediate b, which is 9.32 kcal mol⁻¹ more stable than the separate reactants, via transition state TS_{a-b} with a barrier of 28.52 kcal mol⁻¹. In TS_{a-b}, the lengths of C₁-O₃, C₄-H₅, and O₃-H₅ bonds are 1.799, 1.141, and 1.623 Å, respectively. These geometrical parameters along with the normal mode corresponding to the imaginary frequency (437i cm⁻¹) of TS_{a-b} clearly indicate that H₅ is migrating from C₄ to O₃ while C₁-O₃ bond is breaking. The migration of H₅ can be attributed to the larger electronegativity of O₃ than C₄, whereas the breaking of C₁-O₃ bond is clearly the result of the nucleophilic attack of Cl⁻ anion on C₁.

When CO₂ enters into the reaction system, a new complex c is formed through a electrostatic attraction between O₃ and C₇, as indicated by the large O₃-C₇ distance (2.739 Å) and small energy release (2.30 kcal mol⁻¹) from this process. Once c is formed, the electrophilic attack of CO₂ to O₃ atom occurs; as a result, C₇-O₃ bond forms and H₅ migrates back to C₄, to produce chloroalkoxy carbonate intermediate d, which lies below the reactants by 18.54 kcal mol⁻¹. This step proceeds via transition state TS_{c-d} with a barrier of 7.16 kcal mol⁻¹, where the lengths of the forming O₃-C₇ and C₄-H₅ bonds are 1.983 and 1.258 Å and the breaking O₃-H₅ distance is 1.331 Å. The imaginary frequency is 435i cm⁻¹ and the normal mode mainly corresponds to large-amplitude motions of H₅, O₃, and C₇ in the desired directions. Subsequently, intermediate d converts into productlike intermediate e via an intramolecular cyclic SN₂-

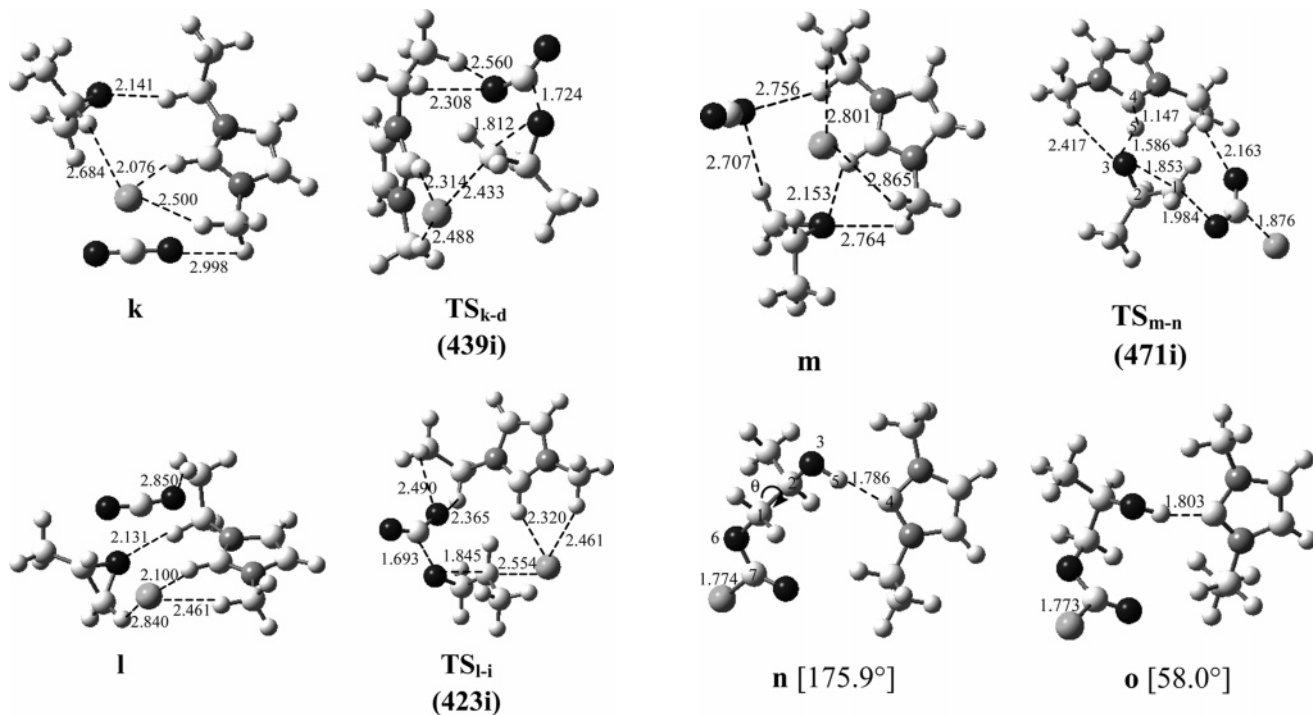


Figure 5. Optimized geometries for the intermediates and transition states exclusively involved in paths III and IV. Values in parentheses denote the imaginary frequencies of transition states. Distances are in angstroms.

type reaction, as demonstrated by transition state TS_{d-e}, where Cl⁻ is getting away from C₁ due to the attack of O₆ from the back. The frequency calculation on TS_{d-e} gives one imaginary frequency of 439i cm⁻¹, and the corresponding transition vector is associated with the formation of C₁-O₆ bond and the breaking of C₁-Cl bond. As shown in Figure 3, in TS_{d-e} the forming C₁-O₆ bond is 1.852 Å, while the breaking C₁-Cl bond is 2.383 Å. The barrier of this SN₂-type reaction is 20.88 kcal mol⁻¹ (see Figure 7). In addition, the productlike intermediate e is found to be more stable in energy by 23.11 kcal mol⁻¹ than the reactants, and its direct dissociation results in the formation of PC and the release of [C₂mim]Cl, and thereby a catalytic cycle is completed. The total reaction is calculated to be exothermic by 23.11 kcal mol⁻¹ compared to the separate reactants, indicating that the channel is thermodynamically favorable.

From Figure 7, it is clear that the cycloaddition reaction in path I now involves a three-step mechanism and the rate-determining step is the first step with a barrier of 28.52 kcal mol⁻¹, which is easily overcome at the experimental temperature of 100 °C²⁴ and is in contrast with the uncatalyzed reaction involving one elementary step with barriers as high as 59.71 and 55.10 kcal mol⁻¹. This fact demonstrates that with the presence of [C₂mim]Cl the reaction mechanism has been modified and the barrier to be surmounted has been reduced remarkably. The important promotion of [C₂mim]Cl for the reaction is ascribed to the concerted effort of [C₂mim]⁺ and Cl⁻ to open the ring of PO via the H-bonding interaction with PO and the nucleophilic attack to PO, respectively, as shown by the vibrational mode of the imaginary frequency and the structural parameters in TS_{a-b} (Figure 3). It is noted that path I is slightly different from the mechanism reported by Park et al.²⁴ Our calculations propose that the nucleophilic attack of Cl⁻ leads to ring opening of PO and thereby the abstraction of H atom from C₄ of [C₂mim]⁺ to O₃, while in the description of Park et al.,²⁴ the H migration process was not proposed. We ascribe this fact to the acidity of the H atom on C₄ of [C₂mim]⁺ and the larger electronegativity of O₃ atom than C₄ atom. It is noteworthy that all intermediates and transition states located

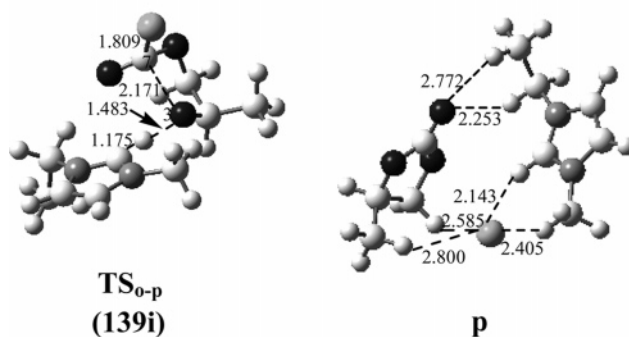


Figure 6. Optimized geometries for the intermediates and transition states involved in path V. Values in parentheses and brackets denote the imaginary frequencies of transition states and the dihedral angles of D_{O3-C2-C1-O6}, respectively. Distances are in angstroms.

in path I involve H-bonding interactions, which play an important role in stabilizing these structures and taking the reaction to the energetically favorable path.

As shown in Figures 4 and 7, path II is an analogue of path I. The main difference between two paths is the initial attack of Cl⁻ on C₁ in path I or C₂ in path II of PO, resulting in the ring opening of PO by breaking C₁-O₃ or C₂-O₃ bond, respectively. The following process to form the product is almost the same with path I. For simplification, here we only show the optimized structures (Figure 4) and draw the PES profile along this path (Figure 7); the relevant details of the geometries, energies, and mechanism are not involved. Compared with path I, the barrier of the rate-determined step in path II is higher by 1.33 kcal mol⁻¹ due to the larger steric hindrance of the methyl group on C₂. This tendency is expected to become more obvious with augmentation of the substitutional group on C₂ in PO. Thus, path II may be not preferred for PO with a large substitutional group, although it is competitive with path I in the present case.

In contrast with the three-step mechanism discussed above, we have also located three two-step paths (III-V in Figure 7) for the cycloaddition reaction, which start from trimolecule complexes k, l, and m (Figures 5 and 6) with similar stabilities (lying below the reactants by 7.11 or 9.80 kcal mol⁻¹) and different relative orientations among CO₂, PO, and [C₂mim]Cl. Paths III and VI are alike in mechanism, which cross into paths I and II via TS_{k-d} and TS_{l-i}, respectively. In TS_{k-d}/TS_{l-i} the C

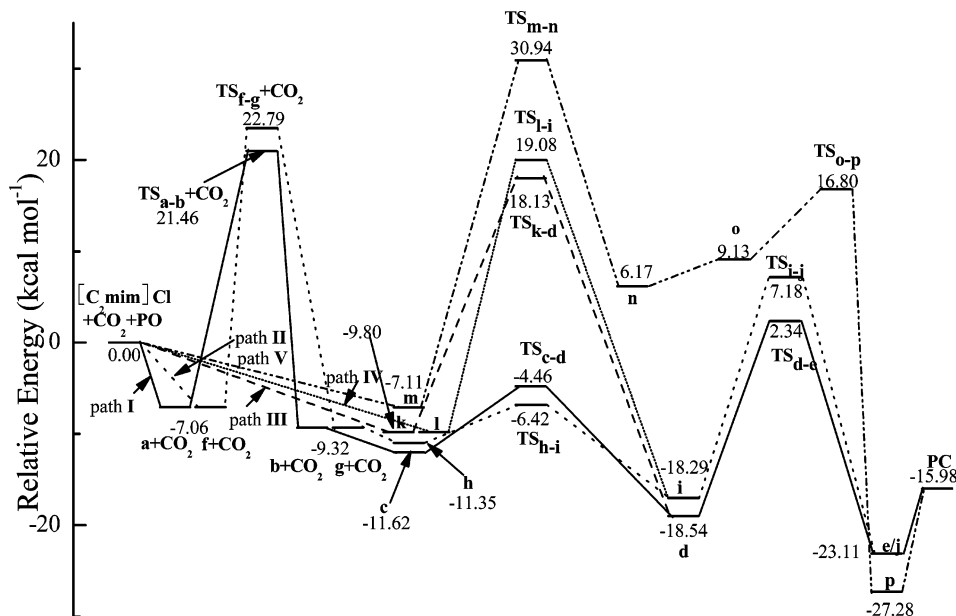


Figure 7. Potential energy surface profiles for the cycloaddition reaction along paths I (—), II (---), III (— · —), IV (····), and V (— · — · —).

atom in CO₂ is joining itself to the O atom in PO as an induced result of the nucleophilic attack of Cl⁻ to the C₁/C₂ atom in PO. The imaginary frequencies of TS_{k-d} and TS_{l-i} are 439i and 423i cm⁻¹, and IRC calculations from these two transition states indicate that they connect intermediates k and d, and l and i, respectively. The sequential processes after i and d along paths III and IV will be not taken into account again because they have been discussed in detail above. From Figure 7, it is clear that the first step along both paths III and IV is the rate-determining step. The barriers from k to TS_{k-d} and from l to TS_{l-i} are found to be 27.93 and 28.88 kcal mol⁻¹, which are comparable with those for the rate-determining steps along paths I and II, 28.52 and 29.85 kcal mol⁻¹. This proposes that paths III and IV are competitive with paths I and II for the cycloaddition reaction.

In the four paths discussed above, Cl⁻ attacks the C atoms on the ring of PO. Now we consider an alternative process, in which Cl⁻ attacks the C atom in CO₂. This conjecture is based on the fact that the C atom of CO₂ carries more positive charge than the C atoms on the ring of PO. As shown by the NBO analysis, the charge on the former is 1.014 au, while that on the latter is from -0.164 to 0.038 au. According to this idea, we have discovered path V for the cycloaddition reaction. Figure 6 shows the four intermediates, m, n, o, and p, and two transition states, TS_{m-n} and TS_{o-p}, involved in this path, and the PES profile is gathered in Figure 7 again. First, the nucleophilic attack of the O atom of CO₂ to C₁ induced by the nucleophilic attack of Cl⁻ to the C atom of CO₂ results in the ring opening of PO and proton migration from C₄ to O₃. This scene is very clear by observing the vivid transition vectors corresponding to the imaginary frequency of TS_{m-n} (471i). By performing IRC calculations in both directions, we found that TS_{m-n} connects m and n. The former is an initial complex among CO₂, PO, and [C₂mim]Cl, which is energetically less favorable by 2.69 kcal mol⁻¹ than k and l. The latter is a metastable intermediate, which lies above the reactants by 6.17 kcal mol⁻¹. The barrier to be overcome from m to n is calculated to be 38.05 kcal mol⁻¹. To obtain the desired product PC, the addition of O₃ to C₇, followed by the departure of Cl⁻ and the migration of H₅ back to C₄, must occur subsequently. However, O₃ and C₇ atoms in n are too far away to realize the addition, so n must distort the dihedral angle of D_{O₃-C₂-C₁-O₆ (175.9°) to form another proper metastable intermediate o (58.0°), which is calculated to be 2.96 kcal mol⁻¹ less stable than n. Although the transition-state structure connecting n and o was not located in the present work,}

we expect that the barrier from n to o is small since this process involves primarily a torsional deformation, rather than bond breaking and bond formation. After intermediate o, the desired addition proceeds via TS_{o-p}, which is 14.14 kcal mol⁻¹ lower than TS_{m-n}, to obtain a productlike intermediate p that has different relative orientation between PC and catalyst with e and j. As shown in Figure 7, the barrier for the rate-determining step along path V is 38.05 kcal mol⁻¹, which is energetically less favorable by about 10 kcal mol⁻¹ than the other four paths. So it is only a possible path for the cycloaddition reaction under high energetics.

To sum up the above discussion, we have located five possible paths for the cycloaddition reaction in the presence of [C₂mim]Cl. Along each path, the reaction proceeds via a stepwise mechanism with much less barrier compared to the uncatalyzed process. The rate-determining steps along all five paths involve consistently the initial ring opening of PO. We found that H-bonding interaction exists throughout all intermediates and transition states, and in most cases it occurs between H₅ atom of [C₂mim]⁺ and O₃ atom of PO due to relatively stronger Lewis acidity of H₅.⁵¹⁻⁵⁴ The notable catalytic activity of [C₂mim]Cl may originate from the cooperative actions of the cation and anion, which stabilize the intermediates and transition states through the hydrogen-bonding interactions and make the ring opening easier via the nucleophilic attack to PO, respectively. It should be noted that our calculations were performed with one Cl⁻ anion, one imidazolium cation, and one each of the two neutral reactants in gas phase, which is different from the real ionic liquid state. The barriers are likely to change if more ion pairs of the ionic liquid system are modeled, although the main conclusions drawn out from the present calculations are expected to hold.

Furthermore, to understand the effects of cation structure on the conversion of PO, we also performed the PES scans for the cycloaddition reaction promoted by [C₄mim]Cl and [C₆mim]Cl along two representative paths, I for the three-step mechanism and III for the two-step mechanism, respectively. The relevant geometries are shown in Figures S1-S4 of the Supporting Information, and the calculated barriers for each elementary step are compared in Table 1 with the corresponding ones in the presence of [C₂mim]Cl. It is found that the barrier of each elementary step slightly decreases with the enlarging cation, with an exception for the second step along path I. However, the tendency is insensitive to the length of the alkyl side chain. The barriers vary at most by about 1 kcal mol⁻¹, which is even

TABLE 1: Calculated Barriers for the Element Steps Involved in the Cycloaddition Reaction of CO₂ with PO in the Presence of [C_nmim]Cl (n = 2, 4, and 6) along Paths I and III

	ΔE , kcal mol ⁻¹		
	[C ₂ mim]Cl	[C ₄ mim]Cl	[C ₆ mim]Cl
	Path I		
ΔE_1^a	28.52	28.35	28.21
ΔE_2^b	7.16	7.31	7.20
ΔE_3^c	20.88	19.72	19.68
	Path III		
ΔE_1^d	27.90	27.59	26.75
ΔE_2^e	20.88	19.72	19.68

^a For the first step (the rate-determining step) along path I. ^b For the second step along path I. ^c For the third step along path I. ^d For the first step (the rate-determining step) along path III. ^e For the second step along path III.

smaller than the error bars of the present B3PW91/6-31G(d,p) calculations. Hence, we conjecture that the experimentally observed trends, that is, the yield of cyclic carbonate increased with lengthening alkyl chain, must be due to bulk solvent effects, which are not taken into account in the present calculations.

4. Conclusions

In this paper, we have carried out a detailed theoretical study for the cycloaddition of CO₂ with PO catalyzed by [C_nmim]Cl (n = 2, 4, and 6). On the basis of the above discussions, the following conclusions can be drawn out.

(i) Compared to the uncatalyzed reaction, the mechanism for the cycloaddition reaction in the presence of [C_nmim]Cl (n = 2, 4, and 6) has been modified, and the barrier of the rate-determining step is reduced by about 20–30 kcal mol⁻¹, clearly indicating that [C_nmim]Cl plays a role of catalyst in the reaction.

(ii) The cycloaddition reaction in the presence of [C_nmim]Cl is a multipath reaction, and it could proceed via five or more possible pathways. In all cases considered in the present work, the rate-determining steps involve the ring opening of PO. According to the present calculations, the three-step paths (paths I and II) are competitive with the two-step paths (paths III and IV), in contrast, another two-step path (path V) may be available only under high energetics.

(iii) The notable catalytic activity of [C₂mim]Cl may originate from the cooperative actions of the cation and anion, which stabilize the intermediates and transition states through the hydrogen-bonding interaction and make the ring opening easier via the nucleophilic attack to PO, respectively.

(iv) The barriers of the cycloaddition reaction are insensitive to the length of the alkyl side chain, and hence the experimentally observed trends, that is, the yield of cyclic carbonate increased with lengthening alkyl chain, must be due to bulk solvent effects.

The present DFT study provides a clear profile for the detailed reaction mechanism and a reasonable explanation for the experimental observations.

Acknowledgment. This work described in this paper is supported by the National Natural Science Foundations of China (Grant 20473047).

Supporting Information Available: Relevant geometries in the presence of [C₄mim]Cl and [C₆mim]Cl along paths I and III. This material is available free of charge via the Internet at <http://pubs.acs.org>.

References and Notes

(1) Chiappe, C.; Pieraccini, D. *J. Phys. Org. Chem.* **2005**, *18*, 275–297.

- (2) Seddon, K. R. *J. Chem. Technol. Biotechnol.* **1997**, *68*, 351–356.
 (3) Jain, N.; Kumar, A.; Chauhan, S.; Chauhan, S. M. S. *Tetrahedron* **2005**, *61*, 1015–1060.
 (4) Welton, T. *Chem. Rev.* **1999**, *99*, 2071–2083.
 (5) Bourbigou, H. O.; Magna, L. J. *Mol. Catal. A: Chem.* **2002**, *182–183*, 419–437.
 (6) Wasserscheid, P.; Welton, T., Eds. *Ionic Liquids in Synthesis*; Wiley-VCH: Weinheim, Germany, 2003.
 (7) Yadav, J. S.; Reddy, B. V. S.; Basak, A. K.; Narsaiah, A. V. *Chem. Lett.* **2003**, *32*, 988–989.
 (8) Peng, J. J.; Deng, Y. Q. *Petrochem. Technol.* **2001**, *30*, 91–93.
 (9) Jiang, T.; Gao, H. X.; Han, B. X.; Zhao, G. Y.; Chang, Y. H.; Wu, W. Z.; Gao, L.; Yang, G. Y. *Tetrahedron Lett.* **2004**, *45*, 2699–2701.
 (10) Boon, J. A.; Levinsky, J. A.; Pflug, J. L.; Wilkes, J. S. *J. Org. Chem.* **1986**, *51*, 480–483.
 (11) Sheldon, R. *Chem. Commun.* **2001**, 2399–2407.
 (12) Zhao, D. B.; Wu, M.; Kou, Y.; Min, E. *Catal. Today* **2002**, *74*, 157–189.
 (13) Lee, S. G. *Chem. Commun.* **2006**, 1049–1063.
 (14) Howarth, J.; Hanlon, K.; Fayne, D.; McCormac, P. *Tetrahedron Lett.* **1997**, *38*, 3097–3100.
 (15) Li, M.; Guo, W. S.; Wen, L. R.; Li, Y. F.; Yang, H. Z. *J. Mol. Catal. A: Chem.* **2006**, *258*, 133–138.
 (16) Shen, H. Y.; Judeh, Z. M. A.; Ching, C. B. *Tetrahedron Lett.* **2003**, *44*, 981–983.
 (17) Ranu, B. C.; Banerjee, S. *J. Org. Chem.* **2005**, *70*, 4517–4519.
 (18) Sun, H.; Zhang, D. J.; Ma, C.; Liu, C. B. *Int. J. Quantum Chem.* **2007**, *107*, 1875–1885.
 (19) Sun, H.; Zhang, D. J.; Wang, F.; Liu, C. B. *J. Phys. Chem. A* **2007**, *111*, 4535–4541.
 (20) Shaikh, A. A. G.; Sivaram, S. *Chem. Rev.* **1996**, *96*, 951–976.
 (21) Parrish, J. P.; Salvatore, R. N.; Jung, K. W. *Tetrahedron* **2000**, *56*, 8207–8237.
 (22) Peng, J. J.; Deng, Y. Q. *New J. Chem.* **2001**, *25*, 639–641.
 (23) Kawanami, H.; Sasaki, A.; Matsui, K.; Ikushima, Y. *Chem. Commun.* **2003**, 896–897.
 (24) Park, D. W.; Mun, N. Y.; Kim, K. H.; Kim, I.; Park, S. W. *Catal. Today* **2006**, *115*, 130–133.
 (25) Kihara, N.; Hara, N.; Endo, T. *J. Org. Chem.* **1993**, *58*, 6198–6202.
 (26) Iwasaki, T.; Kihara, N.; Endo, T. *Bull. Chem. Soc. Jpn.* **2000**, *73*, 713–719.
 (27) Yano, T.; Matsui, H.; Koike, T.; Ishiguro, H.; Fujihara, H.; Yoshihara, M.; Maeshima, T. *Chem. Commun.* **1997**, 1129–1130.
 (28) Yamaguchi, K.; Ebitani, K.; Yoshida, T.; Yoshida, H.; Kaneda, K. *J. Am. Chem. Soc.* **1999**, *121*, 4526–4527.
 (29) Nomura, R.; Ninagawa, A.; Matsuda, H. *J. Org. Chem.* **1980**, *45*, 3735–3738.
 (30) Kim, H. S.; Kim, J. J.; Lee, B. G.; Jung, O. S.; Jang, H. G.; Kang, S. O. *Angew. Chem., Int. Ed.* **2000**, *39*, 4096–4098.
 (31) Paddock, R. L.; Nguyen, S. T. *J. Am. Chem. Soc.* **2001**, *123*, 11498–11499.
 (32) Sun, J.; Wang, L.; Zhang, S. J.; Li, Z. X.; Zhang, X. P.; Dai, W. B.; Mori, R. *J. Mol. Catal. A: Chem.* **2006**, *256*, 295–300.
 (33) Daskocil, E. J.; Bordawekar, S. V.; Kaye, B. G.; Davis, R. J. *J. Phys. Chem. B* **1999**, *103*, 6277–6282.
 (34) Becke, A. D. *Phys. Rev. A* **1988**, *38*, 3098–3100.
 (35) Lee, C.; Yang, W. T.; Parr, R. G. *Phys. Rev. B* **1988**, *37*, 785–789.
 (36) Perdew, J. P.; Wang, Y. *Phys. Rev. B* **1992**, *45*, 13244–13249.
 (37) Becke, A. D. *J. Chem. Phys.* **1993**, *98*, 5648–5652.
 (38) Perdew, J. P.; Burke, K.; Wang, Y. *Phys. Rev. B* **1996**, *54*, 16533–16539.
 (39) Frisch, M. J.; Trucks, G. W.; Schlegel, H. B.; Scuseria, G. E.; Robb, M. A.; Cheeseman, J. R.; Montgomery, J. A., Jr.; Vreven, T.; Kudin, K. N.; Burant, J. C.; Millam, J. M.; Iyengar, S. S.; Tomasi, J.; Barone, V.; Mennucci, B.; Cossi, M.; Scalmani, G.; Rega, N.; Petersson, G. A.; Nakatsuji, H.; Hada, M.; Ehara, M.; Toyota, K.; Fukuda, R.; Hasegawa, J.; Ishida, M.; Nakajima, T.; Honda, Y.; Kitao, O.; Nakai, H.; Klene, M.; Li, X.; Knox, J. E.; Hratchian, H. P.; Cross, J. B.; Bakken, V.; Adamo, C.; Jaramillo, J.; Gomperts, R.; Stratmann, R. E.; Yazyev, O.; Austin, A. J.; Cammi, R.; Pomelli, C.; Ochterski, J. W.; Ayala, P. Y.; Morokuma, K.; Voth, G. A.; Salvador, P.; Dannenberg, J. J.; Zakrzewski, V. G.; Dapprich, S.; Daniels, A. D.; Strain, M. C.; Farkas, O.; Malick, D. K.; Rabuck, A. D.; Raghavachari, K.; Foresman, J. B.; Ortiz, J. V.; Cui, Q.; Baboul, A. G.; Clifford, S.; Cioslowski, J.; Stefanov, B. B.; Liu, G.; Liashenko, A.; Piskorz, P.; Komaromi, I.; Martin, R. L.; Fox, D. J.; Keith, T.; Al-Laham, M. A.; Peng, C. Y.; Nanayakkara, A.; Challacombe, M.; Gill, P. M. W.; Johnson, B.; Chen, W.; Wong, M. W.; Gonzales, C.; Pople, J. A. *Gaussian 03*, Revision D.01; Gaussian, Inc.: Wallingford CT, 2004.
 (40) Milet, A.; Korona, T.; Moszynski, R.; Kochanski, E. *J. Chem. Phys.* **1999**, *111*, 7727–7735.

- (41) Aggarwal, A.; Lancaster, N. L.; Sethi, A. R.; Welton, T. *Green Chem.* **2002**, *4*, 517–520.
- (42) Huang, J. F.; Chen, P. Y.; Sun, I. W.; Wang, S. P. *Inorg. Chim. Acta* **2001**, *320*, 7–11.
- (43) Ross, J.; Xiao, J. L. *Chem.—Eur. J.* **2003**, *9*, 4900–4906.
- (44) Hunt, P. A.; Gould, I. R. *J. Phys. Chem. A* **2006**, *110*, 2269–2282.
- (45) Chang, H. C.; Jiang, J. C.; Tsai, W. C.; Chen, G. C.; Lin, S. H. *J. Phys. Chem. B* **2006**, *110*, 3302–3307.
- (46) Fukui, K. *J. Phys. Chem.* **1970**, *74*, 4161–4163.
- (47) Reed, A. E.; Weinstock, R. B.; Weinhold, F. *J. Chem. Phys.* **1985**, *83*, 735–746.
- (48) Reed, A. E.; Curtiss, L. A.; Weinhold, F. *Chem. Rev.* **1988**, *88*, 899–926.
- (49) *Handbook of Chemistry and Physics*; Lide, D. R., Ed.; CRC Press: Boca Raton, FL, 1995.
- (50) Swalen, J. D.; Herschbach, D. R. *J. Chem. Phys.* **1957**, *27*, 100–108.
- (51) Holbrey, J. D.; Reichert, W. M.; Nieuwenhuyzen, M.; Johnston, S.; Seddon, K. R.; Rogers, R. D. *Chem. Commun.* **2003**, 1636–1637.
- (52) Sun, X. W.; Zhao, S. Q.; Wang, R. A. *Chin. J. Catal.* **2004**, *3*, 247–251.
- (53) Magill, A. M.; Yates, B. F. *Aust. J. Chem.* **2004**, *57*, 1205–1210.
- (54) Saha, S.; Hayashi, S.; Kobayashi, A.; Hamaguchi, H. *Chem. Lett.* **2003**, *32*, 740–741.